ISSN 1070-3284, Russian Journal of Coordination Chemistry, 2018, Vol. 44, No. 10, pp. 604–612. © Pleiades Publishing, Ltd., 2018.
Original Russian Text © O.V. Loseva, T.A. Rodina, A.V. Ivanov, I.A. Lutsenko, E.V. Korneeva, A.V. Gerasimenko, A.I. Smolentsev, 2018, published in Koordinatsionnaya Khimiya, 2018, Vol. 44, No. 5, pp. 303–311.

Heteroleptic Dithiocarbamato–Chlorido Gold(III) Complexes $[Au(S_2CNR_2)Cl_2]$ ($R = CH_3$, *iso*-C_3H_7; $R_2 = (CH_2)_6$): Synthesis, Supramolecular Structures, and Thermal Behavior

O. V. Loseva[a], T. A. Rodina[b], A. V. Ivanov[a, *], I. A. Lutsenko[c], E. V. Korneeva[a], A. V. Gerasimenko[d], and A. I. Smolentsev[e, f]

[a] *Institute of Geology and Nature Management, Far East Branch, Russian Academy of Sciences, Blagoveshchensk, 675000 Russia*

[b] *Amur State University, Blagoveshchensk, 675027 Russia*

[c] *Kurnakov Institute of General and Inorganic Chemistry, Russian Academy of Sciences, Moscow, 119991 Russia*

[d] *Institute of Chemistry, Far East Branch, Russian Academy of Sciences, Vladivostok, 690022 Russia*

[e] *Nikolaev Institute of Inorganic Chemistry, Siberian Branch, Russian Academy of Sciences, Novosibirsk, 630090 Russia*

[f] *Novosibirsk State University, Novosibirsk, 630090 Russia*

**e-mail: alexander.v.ivanov@chemist.com*

Received December 27, 2017

Abstract—The chemisorption binding of gold(III) by freshly precipitated binuclear zinc dithiocarbamates $[Zn_2(S_2CNR_2)_4]$ from solutions in 2 M HCl makes it possible to obtain heteroligand complexes $[Au(S_2CNR_2)Cl_2]$: $R = CH_3$ (**I**), *iso*-C_3H_7 (**II**); $R_2 = (CH_2)_6$ (**III**). The structural organization of complexes **I**, **II**, and **III** is determined by X-ray diffraction analysis (CIF files CCDC no. 1813107, 1813369, and 1813108, respectively). The distorted square–planar structure of the *cis*-$[AuS_2Cl_2]$ chromophores shows the low-spin dsp^2-hybrid state of the central gold atom. Pairwise secondary interactions Au···S between the adjacent molecules in complexes **I** and **III** result in the building of zigzag polymer chains $(\cdots[Au\{S_2CN(CH_3)_2\}Cl_2]\cdots)_n$ and binuclear aggregates $[Au\{S_2CN(CH_2)_6\}Cl_2]_2$ at the supramolecular level. Complex **II** is presented by discrete molecules $[Au\{S_2CN(iso\text{-}C_3H_7)_2\}Cl_2]$. According to the simultaneous thermal analysis data, the single final product of the thermolysis of compounds **I–III** is reduced elemental gold.

Keywords: complex-chemisorbents, forms of gold binding from solutions, heteroleptic dithiocarbamato–chlorido gold(III) complexes, supramolecular self-organization, secondary interactions Au···S, simultaneous thermal analysis

DOI: 10.1134/S107032841810007X

INTRODUCTION

Heteroleptic dialkyl dithiocarbamato-chlorido (and -bromido) complexes of gold(III) are of practical interest because of their high cytotoxic properties, which is significant for the preparation of efficient antitumor and anticancer drugs of the new generation [1–6]. In addition, possibilities of using the gold(III) and gold(I) complexes containing dithiocarbamate ligands in medicine and technology (as sensors of volatile chemical agents [7]) are discussed [7–11]. The following platinum(II) compounds are used for the treatment of human oncological diseases during several decades: cisplatin (first generation), carboplatin (second generation), and oxaliplatin (third generation). The distorted square–planar gold(III) complexes $[Au(S_2CNR_2)Cl_2]$ structurally similar to cisplatin and containing two chlorine atoms *cis*-coordinating to the metal center, which is isoelectronic to platinum(II), are presently considered as promising antitumor drugs [1–6]. The selectivity of the gold(III) dithiocarbamatohalide complexes to cancer cells was established in the recent years. Therefore, the synthesis of new complexes of this type and determination of their structural organization and physicochemical properties are urgent tasks.

Earlier, when studying the chemisorption properties of the zinc and cadmium dithiocarbamate complexes toward solutions of $AuCl_3$ in 2 M HCl, we obtained the heteroligand crystalline complexes

$[Au(S_2CNR_2)Cl_2]_n$ ($R_2 = (CH_2)_5$ [12, 13[1]], $R = C_2H_5$ [14, CIF file CCDC no. 942470][2]) and characterized them by the data of ^{13}C MAS NMR, X-ray diffraction analysis, and simultaneous thermal analysis (STA). The structures of the compounds exhibit the formation of zigzag polymer chains. Molecules of the complexes with the antiparallel orientation linked by pairs of secondary bonds Au···S alternate along the chains. The low-temperature modification of the $[Au\{S_2CN(C_2H_5)_2\}Cl_2]$ complex includes two types of nonequivalent molecules: A and B. Each modification forms an independent polymer chain $(\cdots A\cdots A\cdots A\cdots)_n$ and $(\cdots B\cdots B\cdots B\cdots)_n$. In addition, copper(II) is also characterized by the complexes, whose internal sphere includes the dialkyl dithiocarbamate and halide ligands $[Cu(S_2CNR_2)X_2]^-$ (X = Cl [16], Br [17]).

Continuing these investigations, in the present work we studied the reactions of freshly precipitated binuclear zinc dithiocarbamates $[Zn_2(S_2CNR_2)_4]$ (R = CH_3, *iso*-C_3H_7; $R_2 = (CH_2)_6$) with anions $[AuCl_4]^-$ in a medium of 2 M HCl. The heterogeneous reactions, including the chemisorption binding of gold(III) from solutions and partial ion exchange, afforded the heteroleptic gold(III) complexes: dichloro(*N*,*N*-dimethyldithiocarbamato-*S*,*S*')gold(III) ($[Au\{S_2CN(CH_3)_2\}Cl_2]_n$, **I**), dichlo-ro(*N*,*N*-di-*iso*-propyldithiocarbamato-*S*,*S*')-gold(III) ($[Au\{S_2CN(iso\text{-}C_3H_7)_2\}Cl_2]$, **II**), and dichloro(*N*,*N*-*cyclo*-hexamethylenedithiocarbamato-*S*,*S*')gold(III) ($[Au\{S_2CN(CH_2)_6\}Cl_2]_2$, **III**). The compounds were characterized by IR spectroscopy, X-ray diffraction analysis, and STA.

EXPERIMENTAL

Sodium dimethyl dithiocarbamate $Na\{S_2CN(CH_3)_2\} \cdot xH_2O$ (Aldrich) was used in the synthesis of the zinc complexes. Sodium di-*iso*-propyl dithiocarbamate and sodium *cyclo*-hexamethylenedithiocarbamate were obtained by the reactions of carbon disulfide (Merck) with di-*iso*-propylamine (Merck) and hexamethyleneimine (Aldrich), respectively, in an alkaline medium [18]. The initial zinc complexes $[Zn_2(S_2CNR_2)_4]$ (R = CH_3 [19], *iso*-C_3H_7 [20]; $R_2 = (CH_2)_6$ [21]) were synthesized by the precipitation of Zn^{2+} cations from the aqueous phase with solutions of the corresponding sodium dithiocarbamates. All initial sodium and zinc dithiocarbamates were characterized by the data of IR spectroscopy (KBr, ν/cm^{-1}) as follows:

$Na\{S_2CN(CH_3)_2\} \cdot xH_2O$: 3369 br.s, 2923 m, 2107 m, 1641 w, 1626 m, 1486 s, 1392 w, 1359 s, 1239 s, 1116 s, 1043 m, 962 s, 678 m, 622 m, 567 w, 539 m, 484 m.

$[Zn_2\{S_2CN(CH_3)_2\}_4]$: 2959 w, 2926 m, 1521 s, 1438 m, 1390 s, 1243 s, 1147 s, 1049 m, 1013 w, 973 s, 566 m.

$Na\{S_2CN(iso\text{-}C_3H_7)_2\} \cdot 3H_2O$: 3369 br.s, 3004 w, 2966 m, 2929 m, 1610 m, 1474 w, 1441 vs, 1372 m, 1354 m, 1307 s, 1195 s, 1145 s, 1031 s, 942 s, 903 w, 883 m, 844 m, 785 m, 637 w, 589 m, 524 m.

$[Zn_2\{S_2CN(iso\text{-}C_3H_7)_2\}_4]$: 3003 m, 2971 s, 2932 m, 2872 m, 1554 w, 1484 s, 1446 m, 1370 s, 1326 s, 1192 s, 1143 s, 1118 m, 1037 s, 974 w, 943 m, 906 m, 846 m, 788 m, 623 w, 617 w, 583 m, 528 m, 475 m.

$Na\{S_2CN(CH_2)_6\} \cdot 2H_2O$: 3369 br.s, 2980 m, 2934 s, 2852 m, 2104 m, 1640 w, 1625 m, 1485 s, 1449 w, 1429 w, 1410 s, 1366 m, 1283 w, 1269 w, 1259 m, 1245 w, 1188 s, 1170 m, 1096 m, 1047 m, 1009 w, 975 s, 954 s, 905 m, 851 m, 764 w, 681 m, 623 m, 568 m, 539 m, 492 m, 455 w.

$[Zn_2\{S_2CN(CH_2)_6\}_4]$: 2925 s, 2853 m, 1500 s, 1484 s, 1454 m, 1450 m, 1428 s, 1367 m, 1347 m, 1288 m, 1267 s, 1244 m, 1196 s, 1177 m, 1163 c, 1094 m, 1056 m, 1003 m, 981 s, 958 m, 902 m, 875 w, 850 m, 826 w, 807 w, 749 w, 622 m, 575 m, 474 m.

Syntheses of compounds I–III were carried out by the chemisorption binding of gold(III) from solutions in 2 M HCl with freshly precipitated binuclear zinc dithiocarbamates, $[Zn_2\{S_2CNR_2\}_4]$ (R = CH_3, *iso*-C_3H_7; $R_2 = (CH_2)_6$) via the following reaction:

$$[Zn_2(S_2CNR_2)_4] + 4H[AuCl_4] = [Au(S_2CNR_2)_2][AuCl_4] + 2[Au(S_2CNR_2)Cl_2] + 2ZnCl_2 + 4HCl.$$

Along with the formation of $[Au(S_2CNR_2)Cl_2]$, this heterogeneous reaction is accompanied by the formation of dithiocarbamato-chlorido complexes of the ionic type $[Au(S_2CNR_2)_2][AuCl_4]$, which are also characterized by the ratio Au : Dtc : Cl = 1 : 1 : 2. The structural organization of the latter was determined earlier in [22] (R = *iso*-C_3H_7) and in [23] ($R_2 = (CH_2)_6$). However, the transition $[Au(S_2CNR_2)_2][AuCl_4] \rightarrow 2[Au(S_2CNR_2)Cl_2]$ with the gradual ligand redistribution and averaging of the compositions of the coordination spheres occurs in moderately heated concentrated solutions of the complexes (in a medium of organic solvents) [12].

A solution of $AuCl_3$ (10 mL, in 2 M HCl) containing 128.4, 94.2, or 96.0 mg of gold was poured to 100 mg of freshly precipitated zinc dimethyl dithiocarbamate, di-*iso*-propyl dithiocarbamate, or *cyclo*-hexamethylenedithiocarbamate, respectively. The mixture was magnetically stirred for 1.5 h. The residual content of gold in the solution was determined on an atomic absorption spectrometer (Hitachi, 1 class, model 180–50). The obtained yellow precipitates were filtered off, washed with water, dried on a filter, and dissolved in a minimum volume of methanol (**I**) or

[1] The structural data on this complex were published [13] simultaneously with our data.

[2] The structure of the compound was repeatedly published one year later [15, CIF file CCDC no. 1403956].

acetone (**II**, **III**) on moderate heating. Transparent crystals of compounds **I** (yellow-orange prisms), **II** (yellow prisms), and **III** (yellow plates) for diffraction analysis were obtained by the slow evaporation of the solvents at 30°C. (The substances were repeatedly recrystallized if necessary.)

Compounds **I–III** were characterized by IR spectroscopy (KBr, ν/cm^{-1}) as follows:

I: 2922 m, 1572 s, 1439 m, 1398 s, 1243 m, 1162 m, 1048 m, 969 m, 566 m.

II: 2972 m, 2932 m, 2871 m, 1535 s, 1462 w, 1450 m, 1374 m, 1346 m, 1272 w, 1184 m, 1140 m, 1116 m, 1034 m, 932 w, 905 w, 846 m, 797 m, 620 m, 579 m, 526 w, 470 w.

III: 2931 m, 2855 m, 1545 s, 1441 m, 1353 w, 1284 w, 1269 m, 1201 m, 1178 w, 1160 m, 1094 m, 1005 w, 989 w, 894 w, 825 w, 752 w, 622 m, 562 w.

The IR spectra of the samples in KBr pellets were recorded on an FSM-1201 interference FTIR spectrometer in a frequency range of 400–4000 cm^{-1}. The spectra were processed using the FSpec program (version 4.0.0.2 for Windows, OOO Monitoring, Russia).

X-ray diffraction analyses of single crystals of compounds **I** and **III** were carried out on a Bruker-Nonius X8 Apex CCD diffractometer, and single crystals of complex **II** were analyzed on a Bruker Kappa APEX II diffractometer [24] (MoK_α radiation, $\lambda = 0.71073$ Å, graphite monochromator) at 296(2) for **I**, 200(2) for **II**, and 150(2) K for **III**. Data for compounds **I** and **III** were collected using a standard procedure of φ and ω scanning of narrow frames. Absorption corrections for compounds **I** and **III** were applied empirically (SADABS) [25], and that for compound **II** was applied by the multiscanning method. All structures were determined by a direct method and refined by least squares (for F^2) in the full-matrix anisotropic approximation of non-hydrogen atoms. The positions of hydrogen atoms were calculated geometrically and included into the refinement in the riding model. The data were collected and edited and the unit cell parameters for compounds **I** and **III** or **II** were refined using the SAINT [25] and APEX2 ([25] or [24]) programs, respectively. The calculations on the determination and refinement of the structures of compounds **I** and **III** or **II** were performed using the SHELXTL program package [25] or [26, 27], respectively. The main crystallographic data and results of structure refinement for compounds **I–III** are presented in Table 1. Selected bond lengths and angles are given in Table 2.

The coordinates of atoms, bond lengths, and bond angles for the complexes studied were deposited with the Cambridge Crystallographic Data Centre (CIF files CCDC nos. 1813107 (**I**), 1813369 (**II**), and 1813108 (**III**); deposit@ccdc.cam.ac.uk or http://www.ccdc.cam.ac.uk).

Thermal behavior of compounds I–III was studied by the STA method with the simultaneous detection of the curves of thermogravimetry (TG) and differential scanning calorimetry (DSC). The study was conducted on an STA 449C Jupiter instrument (NETZSCH) in corundum crucibles under a cap with a hole providing a vapor pressure of 1 atm upon the thermal decomposition of the sample. The heating rate was 5°C/min to 1100°C in an argon atmosphere. Recording in aluminum crucibles was additionally used for more distinct revealing thermal effects in the initial region of the DSC curve. The mass of the samples was 3.737–4.254 (**I**), 3.532–3.991 (**II**), and 4.595–5.405 mg (**III**). The accuracy of temperature measurement was ±0.7°C, and that of a weight change was $\pm 1 \times 10^{-4}$ mg. When recording the TG and DSC curves, a correction file was used, as well as temperature and sensitivity calibrations for a given temperature program and heating rate. The independent determination of the melting points of the complexes was carried out on a PTP(M) instrument (OAO Khimlaborpribor, Russia).

After the thermal analysis, the qualitative determination of the chemical composition of the residual substance was conducted by the microprobe method using a RONTEC energy dispersive spectrometer integrated with a LEO-1420 scanning electron microscope.

RESULTS AND DISCUSSION

The reactions of the freshly precipitated complexes $[Zn_2(S_2CNR_2)_4]$ (R = CH_3, *iso*-C_3H_7; $R_2 = (CH_2)_6$) with anions $[AuCl_4]^-$ in 2 M HCl are accompanied by the reformation of bulky clotted precipitates with a decrease in the particle size and a change in the color from white to yellow, indicating the formation of new compounds in the systems studied. The working solutions of gold(III) undergo parallel decoloration: in 15 min the degree of binding of gold from solutions reaches ~98%. The binding of gold calculated from the above presented heterogeneous reaction (see section Synthesis of **I–III**) is 1288.2, 941.2, and 951.5 mg Au^{3+} per 1 g of zinc dithiocarbamates $[Zn_2(S_2CNR_2)_4]$ (R = CH_3, *iso*-C_3H_7, and $R_2 = (CH_2)_6$), respectively.

The chemical and structural identifications of crystalline complexes **I–III** isolated in preparative amounts were performed by IR spectroscopy and X-ray diffraction analysis.

In the IR spectra of compounds **I–III**, single high-intensity absorption bands at 1572 (**I**), 1535 (**II**), and 1545 (**III**) cm^{-1} are assigned to stretching vibrations of the thioureide N–C(S)S group. The range of ν(C–N) values is determined by vibrations of both ordinary (1250–1360 cm^{-1}) and double bonds (1640–1690 cm^{-1}). For complexes **I–III**, the discussed bands arranged between the indicated limiting values are significantly shifted to the high-frequency range, indicating the predominantly double character of the N–C(S)S bond [18, 28, 29]. The systematic and sub-

Table 1. Crystallographic data and experimental and structure refinement parameters for compounds **I–III**

Parameter	Value		
	I	**II**	**III**
Empirical formula	$C_3H_6NS_2Cl_2Au$	$C_7H_{14}NS_2Cl_2Au$	$C_7H_{12}NS_2Cl_2Au$
FW	388.07	444.18	442.16
Crystal system	Monoclinic	Orthorhombic	Triclinic
Space group	$P2_1/m$	*Pnma*	$P\bar{1}$
a, Å	6.6573(6)	14.3243(2)	6.9473(6)
b, Å	6.8907(6)	8.47370(10)	7.6462(7)
c, Å	10.0457(8)	10.4018(2)	11.8954(11)
α, deg	90.00	90.00	83.849(2)
β, deg	108.664(3)	90.00	77.660(2)
γ, deg	90.00	90.00	66.941(2)
V, Å^3	436.60(6)	1262.57(3)	567.78(9)
Z	2	4	2
ρ_{calcd}, g/cm^3	2.952	2.337	2.586
μ, mm^{-1}	17.855	12.365	13.748
F(000)	352	832	412
Crystal size, mm	0.15 × 0.05 × 0.02	0.41 × 0.24 × 0.16	0.20 × 0.14 × 0.02
Range of data collection over θ, deg	2.14–27.53	2.42–35.15	1.75–27.73
Ranges of reflection indices	$-8 \le h \le 8$, $-8 \le k \le 8$, $-13 \le l \le 12$	$-22 \le h \le 22$, $-13 \le k \le 9$, $-16 \le l \le 16$	$-9 \le h \le 4$, $-9 \le k \le 9$, $-15 \le l \le 14$
Measured reflections	4190	19975	4450
Independent reflections (R_{int})	1086 (0.0307)	2945 (0.0321)	2610 (0.0219)
Reflections with $I > 2\sigma(I)$	1024	2535	2471
Refinement variables	57	76	118
GOOF	1.156	1.084	1.046
R_1, wR_2 for $F^2 > 2\sigma(F^2)$	0.0233, 0.0550	0.0167, 0.0394	0.0241, 0.0669
R_1, wR_2 for all reflections	0.0253, 0.0556	0.0219, 0.0418	0.0261, 0.0678
Extinction coefficient		0.00244(15)	
Residual electron density (min/max), *e*/Å^3	−0.741/2.261	−0.835/1.167	−1.527/2.111

stantial shift of the bands of the thioureide group to the range of the C=N bond vibrations is observed for the gold(III) complexes compared to the initial sodium and zinc dithiocarbamates, which shows an increase in the contribution of double bonding to the formally ordinary N–C(S)S bond due to the bidentate chelate coordination of the dithiocarbamate ligands by gold(III) to form Au–S bonds. The medium-intensity absorption bands in ranges of 1140–1162 and 932–989 cm^{-1} were assigned to asymmetric (ν_{as}) and symmetric (ν_s) stretching vibrations of the –C(S)S– group, respectively [30, 31]. Weak bands at 562–622 cm^{-1} are attributed to the ν(C–S) vibrations [32]. The absorption bands caused by the stretching and bending vibrations of the bonds of the alkyl substituents in the Dtc ligands fall onto a range of 2855–2972 cm^{-1}.

The unit cells of the studied compounds contain two (**I**, **III**) or four (**II**) molecules of the heteroleptic complexes $[Au(S_2CNR_2)Cl_2]$ (R = CH_3, *iso*-C_3H_7; $R_2 = (CH_2)_6$) (Fig. 1). All complexes are characterized by the same type of structural organization: in each complex the central gold atom coordinates two chlorine atoms and one dithiocarbamate ligand via the *S*,*S*′-bidentate mode to form chromophores *cis*-$[AuS_2Cl_2]$ (Fig. 2). The distorted square-planar geometry of the latter indicates the low-spin intraorbital dsp^2-hybrid state of the gold atoms. The chlorine atoms exhibit structural nonequivalence: in each

Table 2. Selected bond lengths (*d*) and bond (ω) and torsion (φ) angles in structures **I**, **II**, and **III***

Bond	*d*, Å	Bond	*d*, Å
	I		
Au(1)–S(1)	2.304(2)	S(1)–C(1)	1.739(8)
Au(1)–S(2)	2.302(2)	S(2)–C(1)	1.743(7)
Au(1)–Cl(1)	2.305(2)	N(1)–C(1)	1.289(9)
Au(1)–Cl(2)	2.315(2)	N(1)–C(2)	1.488(10)
Au(1)···S(2)[a]	3.4745(4)	N(1)–C(3)	1.447(11)
	II		
Au(1)–S(1)	2.2944(6)	N(1)–C(1)	1.299(2)
Au(1)–S(2)	2.2783(6)	N(1)–C(2)	1.489(3)
Au(1)–Cl(1)	2.3143(6)	N(1)–C(4)	1.499(3)
Au(1)–Cl(2)	2.3235(6)	C(2)–C(3)	1.518(2)
S(1)–C(1)	1.741(2)	C(4)–C(5)	1.519(2)
S(2)–C(1)	1.732(2)		
	III		
Au(1)–S(1)	2.3003(12)	S(1)–C(1)	1.736(5)
Au(1)–S(2)	2.3023(12)	S(2)–C(1)	1.730(5)
Au(1)···S(1)[a]	3.5736(13)	N(1)–C(1)	1.316(6)
Au(1)–Cl(1)	2.3170(12)	N(1)–C(2)	1.468(6)
Au(1)–Cl(2)	2.3219(12)	N(1)–C(7)	1.484(6)
Angle	ω, deg	Angle	ω, deg
	I		
S(1)C(1)S(2)	109.5(4)	S(2)Au(1)Cl(2)	95.37(7)
S(1)Au(1)S(2)	76.24(7)	Cl(1)Au(1)Cl(2)	91.55(8)
S(1)Au(1)Cl(1)	96.84(8)	Au(1)S(1)C(1)	87.1(2)
S(1)Au(1)Cl(2)	171.61(7)	Au(1)S(2)C(1)	87.1(2)
S(2)Au(1)Cl(1)	173.08(7)		
	II		
S(1)C(1)S(2)	107.49(11)	S(2)Au(1)Cl(2)	93.31(2)
S(1)Au(1)S(2)	75.52(2)	Cl(1)Au(1)Cl(2)	95.68(2)
S(1)Au(1)Cl(1)	95.499(19)	Au(1)S(1)C(1)	88.13(7)
S(1)Au(1)Cl(2)	168.83(3)	Au(1)S(2)C(1)	88.87(7)
S(2)Au(1)Cl(1)	171.02(2)		
	III		
S(1)C(1)S(2)	109.6(3)	Cl(1)Au(1)S(2)	170.91(4)
S(1)Au(1)S(2)	75.98(4)	Cl(2)Au(1)S(1)	170.99(4)
S(1)Au(1)Cl(1)	94.93(4)	Au(1)S(1)C(1)	87.2(2)
Cl(1)Au(1)Cl(2)	93.90(4)	Au(1)S(2)C(1)	87.2(2)
Cl(2)Au(1)S(2)	95.19(4)		
Angle	φ, deg	Angle	φ, deg
	III		
Au(1)S(1)S(2)C(1)	−179.3(3)	S(1)C(1)N(1)C(7)	176.7(4)
S(1)Au(1)C(1)S(2)	−179.4(3)	S(2)C(1)N(1)C(2)	178.1(4)
S(1)C(1)N(1)C(2)	−1.7(7)	S(2)C(1)N(1)C(7)	−3.5(6)

* Symmetry transforms: [a] $1-x, 1/2+y, 1-z$ (**I**); [a] $-x, 2-y, 1-z$ (**III**).

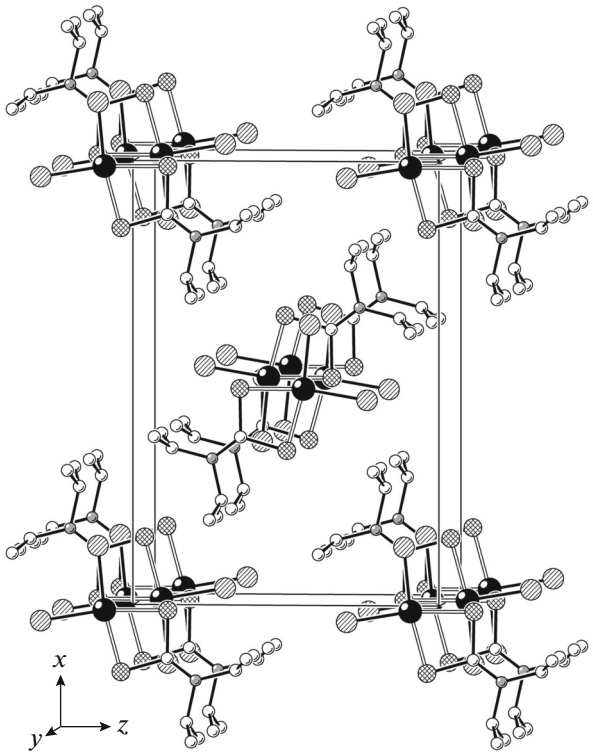

Fig. 1. Projection of the crystal structure of complex **II** onto the *xz* plane.

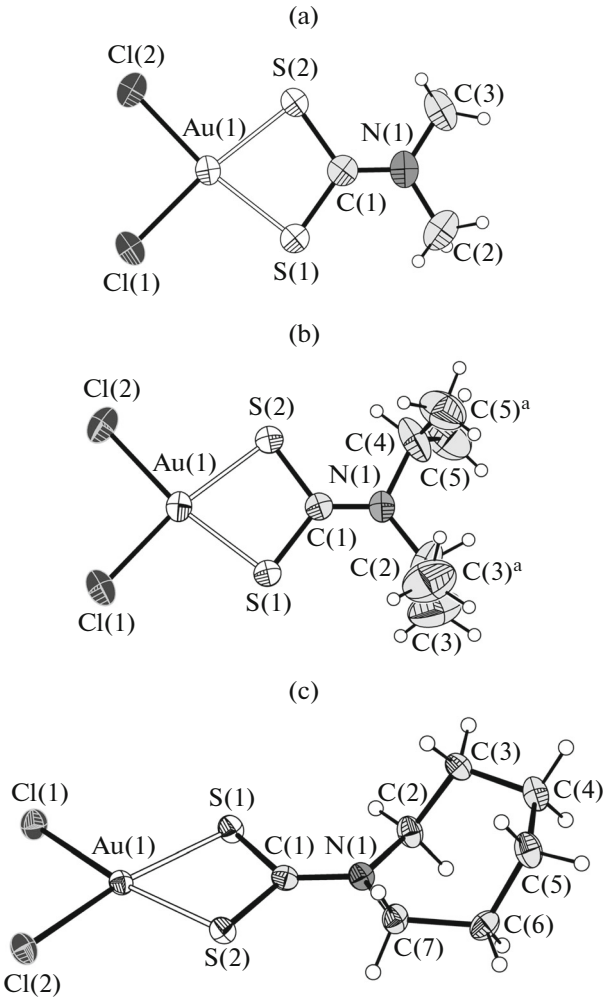

Fig. 2. Molecular structures of complexes (a) **I**, (b) **II**, and (c) **III**. Ellipsoids of 50% probability. Symmetry transform: [a] x, $1/2 - y$, z.

complex one of the Au–Cl bonds is reliably stronger than another (Table 2).

In compounds **I–III**, the Dtc ligands exhibit the coordination mode close to *S*,*S*′-isobidentate (Au–S bond lengths are 2.302, 2.304 (**I**), 2.2783, 2.2944 (**II**), and 2.3003 and 2.3023 Å (**III**)), and the degree of binding in complex **II** is somewhat higher. The coordination discussed is accompanied by the formation of small-size four-membered metallocycles [AuS_2C]: the Au···C distances (2.816, 2.842, and 2.812 Å for **I**, **II**, and **III**, respectively) are much shorter than the sum of the van der Waals radii of these atoms (3.36 Å) [33] and indicate the *trans*-annular interaction between the gold and carbon atoms. The molecules of complexes **I** and **II** (except for the terminal $-CH_3$ groups of the di-*iso*-propyl dithiocarbamate ligand) lie on the mirror reflection plane (*m*), which determines coplanarity of the atoms in the [AuS_2Cl_2] chromophores, [AuS_2C] metallocycles, and $C_2NC(S)S$ groups. The atoms belonging to the [AuS_2C] metallocycles and $C_2NC(S)S$ group in complex **III** somewhat deviate from the plane, which is illustrated by the AuSSC and SAuCS torsion angles that are deviated from 180° and 0° (Table 2). The N–C(S)S bond length (1.289 Å for **I** and 1.299 Å for **II**) is close to the typical value of the C=N double bond (1.27 Å), reflecting the predominantly sp^2-hybrid state of the nitrogen and carbon atoms and the mesomeric effect manifested by the dithiocarbamate groups. The N–C(S)S bond length in complex **III** (1.316 Å) is intermediate between the typically ordinary (1.47 Å) and double (1.27 Å) bonds. A direct consequence of a significant contribution of double bonding to the formally ordinary bonds N–C(S)S is also the effective averaging of the C(1)–S(1) and C(1)–S(2) bond lengths in complexes **I–III**: 1.739, 1.743 (**I**), 1.741, 1.732 (**II**), and 1.736, 1.730 Å (**III**), indicating that the π-electron density is delocalized inside the [AuS_2C] metallocycles.

The pair secondary bonds Au···S[3] play the determining role in the structural organization at the supramolecular level in compounds **I** and **III**. In the first case, the central gold atom and one of the sulfur atoms participate in the interactions with two closest neigh-

[3] The concept of secondary bonds was given [34] for the first time to substantiate interactions between atoms at distances close to the sums of their van der Waals radii.

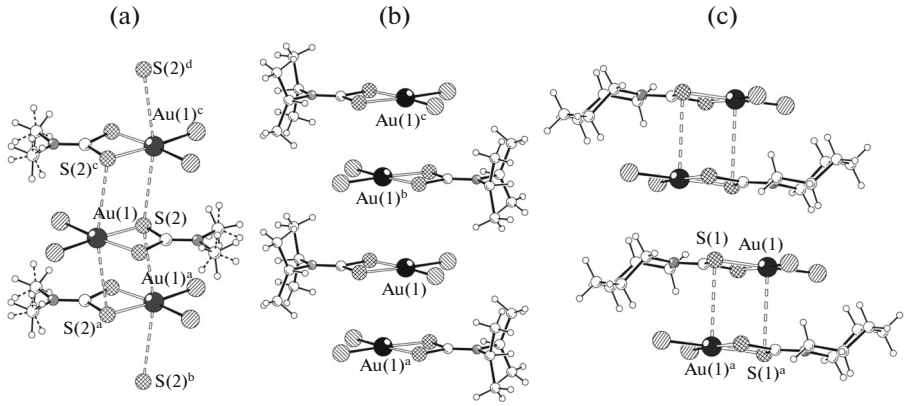

Fig. 3. (a) Fragment of the polymer chain $([Au\{S_2CN(CH_3)_2\}Cl_2])_n$ (**I**), (b) discrete molecules $[Au\{S_2CN(iso\text{-}C_3H_7)_2\}Cl_2]$ (**II**), and (c) binuclear molecules $[Au_2\{S_2CN(CH_2)_6\}_2Cl_4]$ (**III**). Secondary bonds Au···S are shown by dotted lines. Symmetry transforms: [a] $1 - x, 1/2 + y, 1 - z$; [b] $x, 1 + y, z$; [c] $1 - x, y - 1/2, 1 - z$; [d] $x, y - 1, z$.

bors of each $[Au\{S_2CN(CH_3)_2\}Cl_2]$ molecule (Fig. 3a) to form two pair of symmetric secondary bonds Au(1)···S(2)[a/c] and S(2)···Au(1)[a/c] (3.4745 Å), which is rather close to the sum of the van der Waals radii of the sulfur and gold atoms (3.46 Å) [33]. As a result, zigzag polymer chains are formed (angle Au(1)Au(1)Au(1) 103.095°, interatomic distance Au(1)–Au(1) 4.3995 Å), and molecules of complex **I** with the parallel orientation alternate along the chains (Fig. 3a). The molecules of compound **III** form binuclear aggregates $[Au\{S_2CN(CH_2)_6\}Cl_2]_2$ (Fig. 3c) due to pair joining by two symmetric secondary bonds Au(1)···S(1)[a] and Au(1)[a]···S(1) (3.5736 Å), which somewhat exceeds the sum of the van der Waals radii of the gold and sulfur atoms. In the centrosymmetric binuclear molecule discussed, the seven-membered heterocycles $-N(CH_2)_6$ of the dithiocarbamate ligands characterized by the skew chair conformation [35–37] are oriented toward the interdimer space.

The gold atoms in the structures of complexes **I** and **III** build up their environments to distorted octahedral $[AuS_4Cl_2]$ (4 + 2) and distorted square pyramidal $[AuS_3Cl_2]$ (4 + 1) ones, respectively, due to the Au···S secondary bonds. In the structure of compound **II**, the role of secondary interactions of the discussed type is substantially diminished, since the Au–S intermolecular distance is 4.2560(1) Å. It can be accepted that the structure discussed is presented by discrete molecules of $[Au\{S_2CN(iso\text{-}C_3H_7)_2\}Cl_2]$ (Fig. 3b) with the formation of stacks including alternating molecules with the antiparallel orientation along the crystallographic axis *y* (Fig. 1).

The thermal behavior of complexes **I–III** in an argon atmosphere was studied by the STA method with the simultaneous detection of the TG and DSC curves. The studied compounds manifest a similar character of thermal destruction (Fig. 4 presents the TG and DSC curves for complex **I**). In the TG curve, the initial step of the smooth mass loss detected at 120–209°C transits to the steeply descending step of the intensive thermolysis of complex **I** (Fig. 4*a*). The inflection at a point of 265°C divides the step discussed into two regions with a mass loss of 24.48% (209–265°C) and 21.54% (265–340°C). Thus, the main mass loss falls onto the narrow temperature range (~120–340°C), being 46.02, 54.39, and 43.19% for compounds **I**, **II**, and **III**, respectively. The subsequent flat region of the TG curve (340–1100, 355–1100, and 300–1100°C for **I**, **II**, and **III**, respectively) is determined by the smooth desorption of the thermolysis products with a mass loss of 3.58, 2.00, and 12.23% for **I**, **II**, and **III**, respectively. The mass loss before the inflection point in the TG curve is 24.48%, which possibly corresponds to the transformation of $(CH_3)_2NC(S)S^-$ into NCS^- and dissociation of the Au–Cl bonds (calculated mass loss 25.15%). The second region shows the reduction of gold to the elemental state (the experimental mass loss including the region of final desorption is 25.12%, and the calculated value is 24.10%).

The residual weight at 1100°C is 50.40, 43.64, and 44.59% (for **I**, **II**, and **III**, respectively) of the initial value, which is close to the values expected for reduced gold (the calculated values are 50.75, 44.34, and 44.54% for **I**, **II**, and **III**, respectively). When the crucible was opened, fine balls of metallic gold without slag traces were found on the bottom. The energy dispersive spectra confirm the formation of elemental gold as the single thermolysis product of complexes **I–III** (Fig. 4*c*).

Two endothermic effects (weak and pronounced) with extremes at 242.0 and 258.0°C are observed in the low-temperature range of the DSC curve of complex **I**. They are caused by the thermolysis of complex **I** via the first step (Fig. 4*b*). None of them is related to melting of the sample: the independent determination (in a glass capillary) showed indications of the melting of

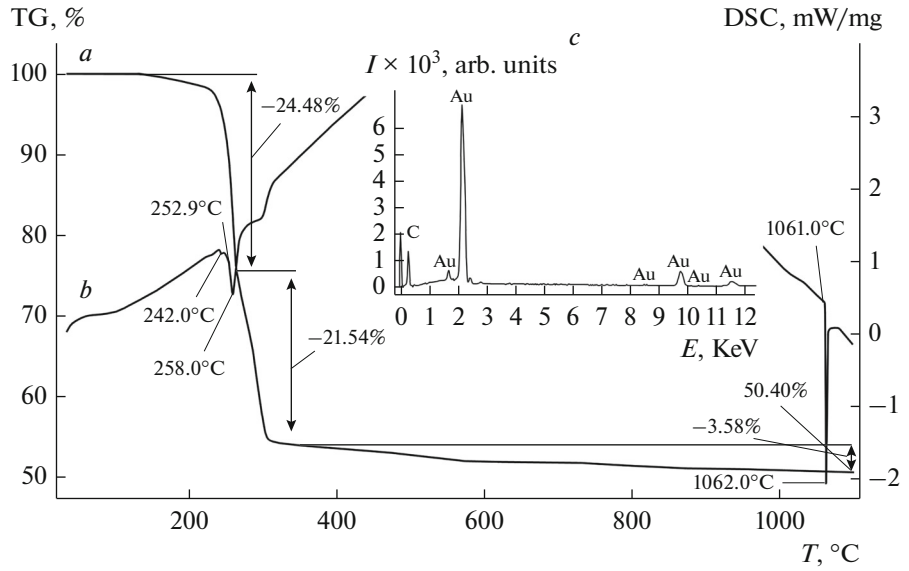

Fig. 4. (*a*) TG and (*b*) DSC curves for complex **I** and (*c*) the energy dispersive spectrum of reduced gold.

the substance with decomposition accompanied by vigorous gas evolution in a range of 248–250°C. The extreme of the first endotherm is projected onto the TG curve at the point (242.0°C) with a mass loss of 3.99%, which can reflect the defragmentation of the dithiocarbamate ligand at the first methyl group as an individual process (calculated mass loss 3.87%). The extreme of the second endotherm coincides with the temperature corresponding to the maximum mass loss rate in the region of the TG curve before the inflection point. The differentiation and double differentiation of the thermal effect manifested as a step in the DSC curve and related to the region of the TG curve after the inflection point did not allow us to reliably reveal its characteristic points. Nevertheless, the extreme is formally determined by the temperature of the maximum rate of mass loss (295.9°C) in the region discussed.

The DSC curve of complex **II** exhibits endotherms with extremes at 191.1 and 288.9°C (the extrapolated temperatures of the corresponding processes are 179.6 and 282.7°C, respectively), the first of which shows the melting of the substance (the independently determined mp is 180°C), and the second extreme corresponds to the thermolysis process. The DSC curve of complex **III** in the low-temperature range also detects two endotherms. To establish the nature of the former (with an extreme at 164.2°C), the sample was additionally studied in an aluminum crucible. The discussed endotherm is not detected repeatedly when recording the sample at temperatures below 190.0°C in the programmed heating–cooling–heating regime, which possibly indicates the transition of the complex to a new crystalline modification. The second endotherm with an extreme at 273.5°C and an extrapolated temperature of 249.6°C falls onto the range of the major mass loss during thermolysis. Since the DSC curve detects no endotherm effect of melting of the complex, the mp of the sample was determined independently (208°C).

The high-temperature DSC range of all studied compounds contains the endotherm of gold melting (Fig. 4*b*), the extrapolated mp of which is 1061.0, 1061.7, and 1061.4°C for complexes **I**, **II**, and **III**, respectively.

ACKNOWLEDGMENTS

This work was supported in part by the Presidium of the Far East Branch of the Russian Academy of Sciences, project no. 15–I–3–001.

REFERENCES

1. Ronconi, L., Giovagnini, L., Marzano, C., et al., *Inorg. Chem.*, 2005, vol. 44, no. 6, p. 1867.
2. Ronconi, L., Marzano, C., Zanello, P., et al., *J. Med. Chem.*, 2006, vol. 49, no. 5, p. 1648.
3. Milacic, V., Chen, D., Ronconi, L., et al., *Cancer Res.*, 2006, vol. 66, no. 21, p. 10478.
4. Chow, K.H.-M., Sun, R.W.-Y., Lam, J.B.B., et al., *Cancer Res.*, 2010, vol. 70, p. 329.
5. Boscutti, G., Feltrin, L., Lorenzon, D., et al., *Inorg. Chim. Acta*, 2012, vol. 393, p. 304.
6. Nardon, C., Boscutti, G., and Fregona, D., *Anticancer Res.*, 2014, vol. 34, no. 1, p. 487.
7. Mansour, M.A., Connick, W.B., and Lachicotte, R.J., *J. Am. Chem. Soc.*, 1998, vol. 120, no. 6, p. 1329.
8. Hogarth, G., *Mini-Rev. Med. Chem.*, 2012, vol. 12, no. 12, p. 1202.
9. Cvek, B. and Dvorak, Z., *Current Pharm. Design*, 2007, vol. 13, no. 30, p. 3155.

10. de Vos, D., Ho, S.Y., and Tiekink, E.R.T., *Bioinorg. Chem. Appl.*, 2004, vol. 2, nos. 1–2, p. 141.
11. Keter, F.K., Guzei, I.A., Nell, M., et al., *Inorg. Chem.*, 2014, vol. 53, no. 4, p. 2058.
12. Rodina, T.A., Ivanov, A.V., Loseva, O.V., et al., *Russ. J. Inorg. Chem.*, 2013, vol. 58, no. 3, p. 338. doi 10.1134/S0036023613030133
13. Shi, Y., Chu, W., Wang, Y., et al., *Inorg. Chem. Commun.*, 2013, vol. 30, p. 178.
14. Rodina, T.A., Ivanov, A.V., and Gerasimenko, A.V., *Russ. J. Coord. Chem.*, 2014, vol. 40, no. 2, p. 100. doi 10.1134/S1070328414020080
15. Altaf, M., Isab, A.A., Vanćo, J., et al., *RSC Adv.*, 2015, vol. 5, p. 81599.
16. Solozhenkin, P.M., Ivanov, A.V., Kopitsya, N.I., and Shvengler, F.A., *Zh. Neorg. Khim.*, 1985, vol. 30, no. 2, p. 416.
17. Solozhenkin, P.M., Ivanov, A.V., Kopitsya, N.I., and Shvengler, F.A., *Zh. Neorg. Khim.*, 1986, vol. 31, no. 10, p. 2573.
18. Byr'ko, V.M., *Ditiokarbamaty* (Dithiocarbamates), Moscow: Nauka, 1984.
19. Klug, H.P., *Acta Crystallogr.*, 1966, vol. 21, no. 4, p. 536.
20. Miyamae, H., Ito, M., and Iwasaki, H., *Acta Crystallogr. Sect. B: Struct. Sci., Crystal Engin., Mater.,* 1979, vol. 35, no. 6, p. 1480.
21. Agre, V.M. and Shugam, E.A., *Zh. Strukt. Khim.*, 1972, vol. 13, no. 4, p. 660.
22. Rodina, T.A., Ivanov, A.V., Gerasimenko, A.V., et al., *Polyhedron*, 2012, vol. 40, no. 1, p. 53.
23. Loseva, O.V., Rodina, T.A., and Ivanov, A.V., *Russ. J. Inorg. Chem.*, 2015, vol. 60, no. 3, p. 307. doi 10.1134/S0036023615030134
24. *APEX2*, Madison: Bruker AXS Inc., 2012.
25. *APEX2 (version 1.08), SAINT (version 7.03), SADABS (version 2.11), SHELXTL (version 6.12)*, Madison: Bruker AXS Inc., 2004.
26. Sheldrick, G.M., *Acta Crystallogr., Sect. A: Found. Adv.*, 2015, vol. 71, no. 1, p. 3.
27. Sheldrick, G.M., *Acta Crystallogr., Sect. C: Struct. Chem.*, 2015, vol. 71, no. 1, p. 3.
28. Fabretti, A.C., Forghieri, F., Giusti, A., et al., *Spectrochim. Acta, Part A*, 1984, vol. 40, no. 4, p. 343.
29. Odola, A.J. and Woods, J.A.O., *J. Chem. Pharm. Res.*, 2011, vol. 3, no. 6, p. 865.
30. Bellamy, L.J., *The Infrared Spectra of Complex Molecules*, New York: Wiley, 1958.
31. Yin, H., Li, F., and Wang, D., *J. Coord. Chem.*, 2007, vol. 60, no. 11, p. 1133.
32. Khitrich, N.V. and Seifullina, I.I., *Koord. Khim.*, 2000, vol. 26, no. 11, p. 848.
33. Winter, M., http://www.webelements.com. Cited January 2010.
34. Alcock, N.W., *Adv. Inorg. Chem. Radiochem.*, 1972, vol. 15, p. 1.
35. Boessenkool, I.K. and Boeyens, J.C.A., *J. Cryst. Mol. Struct.*, 1980, vol. 10, no. 1/2, p. 11.
36. Evans, G. and Boeyens, J.C.A., *Acta Crystallogr. Sect. B: Struct. Sci., Crystal Engin., Mater.,* 1989, vol. 45, no. 6, p. 581.
37. Entrena, A., Campos, J., Gomez, J.A., et al., *Org. Chem.*, 1997, vol. 62, no. 2, p. 337.

Translated by E. Yablonskaya